

Research paper

Integrative analysis of h-prune as a potential therapeutic target for hepatocellular carcinoma


 Haotian Liao^{a,1}, Mingheng Liao^{a,1}, Lin Xu^b, Xiaokai Yan^a, Bo Ren^a, Zexin Zhu^a, Kefei Yuan^{a,b,*}, Yong Zeng^{a,b,*}
^a Department of Liver Surgery, Liver Transplantation Division, West China Hospital, Sichuan University, Chengdu, Sichuan, People's Republic of China

^b Laboratory of Liver Surgery, West China Hospital, Sichuan University, Chengdu, Sichuan, People's Republic of China

ARTICLE INFO

Article history:

Received 5 December 2018

Received in revised form 26 December 2018

Accepted 3 January 2019

Available online 18 January 2019

Keywords:

Hepatocellular carcinoma

Hepatocellular carcinoma

H-prune

Prognosis

Therapeutic target

ABSTRACT

Background: *Drosophila* prune protein (h-prune) has been proved to play an essential role in regulating tumor metastasis. However, the clinical relevance of h-prune and its potential mechanism in regulating hepatocellular carcinoma (HCC) are still poorly understood.

Methods: In this study, we used tissue microarrays (TMA) containing 304 HCC tumor samples to evaluate the expression of h-prune and its correlation with prognosis. Data of RNAseq, mutation profiles, copy number variation (CNV), miRNAseq and methylation array from The Cancer Genome Atlas (TCGA) dataset were adopted to analyze the distinctive genomic patterns associated with h-prune expression.

Results: By using TMA, we found increased expression of h-prune in HCC tumor cells compared with adjacent normal tissues. Higher expression of h-prune was correlated with poorer OS and DFS outcomes. In addition, multivariate analysis showed that h-prune expression was an independent risk factor for both OS and DFS. Gene enrichment analysis showed that the gene signatures of cell proliferation, DNA methylation and canonical Wnt signaling pathway were enriched in h-prune-high patients. Notably, somatic mutation analysis demonstrated that higher mutation burden of RB1 and RPS6KA3 could be observed in h-prune-high patients. Moreover, integrative analysis revealed a strong correlation between h-prune expression and epigenetic changes.

Interpretation: This study has highlighted the clinical value of h-prune in predicting the prognosis of HCC patients and its essential role in promoting tumorigenesis of HCC.

© 2019 The Authors. Published by Elsevier B.V. This is an open access article under the CC BY-NC-ND license (<http://creativecommons.org/licenses/by-nc-nd/4.0/>).

1. Introduction

Hepatocellular carcinoma (HCC) has been ranked as second leading cause of cancer death worldwide, with >4 million new cases diagnosed in 2015 [1]. Over the past decades, while great advances have been achieved in the diagnosis and treatment of HCC, the prognosis for HCC patients still remains poor [2]. Thus, there is an urgent need to find effective prognostic biomarkers for HCC patients who can really benefit from curative treatment. Various biological and molecular events within tumor microenvironment, including somatic mutations, aberrant expression of oncogenes and copy number variations (CNVs), have been identified as significant prognostic biomarkers for HCC [3–5]. It is notable that cancer research nowadays has integrated various molecules into clinical care to predict the survival outcomes of HCC patients, which inspired more studies on the molecular pathology in HCC.

Phosphodiesterases (PDE), an enzyme family that terminates cyclic nucleotide signaling by catalyzing the hydrolysis of cAMP and GMP, have been proved to play potential roles in predisposition to different cancer types, including melanoma, prostate cancer and B-cell malignancies [6–8]. At this moment, studies on cancers have been focusing on the human homolog of *Drosophila* prune protein (h-prune), which belongs to the DHH superfamily of phosphoesterases. It has been shown by previous studies that h-prune can promote tumor metastasis by cooperatively regulating the disassembly of focal adhesions with glycogen synthase kinase 3 (GSK3), and physically interacting with nm23-H1, a metastasis suppressor gene [9,10]. These facts suggest the potential role of h-prune as a prognostic biomarker for patients with cancers. Indeed, it has been reported that higher expression of h-prune is associated with advanced disease status colorectal liver metastases (CLM), breast cancer, medulloblastoma, lung cancer and thyroid cancer [11–15]. However, the prognostic value of h-prune expression and its potential mechanism regulating carcinogenesis in HCC are still poorly understood.

In this study, we used tissue microarrays (TMA) to examine 304 HCC tumor samples and analyzed the distinctive genomic patterns associated with h-prune expression by using data from The Cancer Genome

* Corresponding authors at: Department of Liver Surgery, Liver Transplantation Division, West China Hospital, Sichuan University, Chengdu, Sichuan, People's Republic of China.

E-mail addresses: ykf13@163.com (K. Yuan), zengyong@medmail.com.cn (Y. Zeng).

¹ These authors contributed equally to this work.

Research in context

Evidence before this study

Over the past decades, finding potential therapy target for HCC patients have been paid attentions widely due to the poor prognosis. *Drosophila* prune protein (h-prune), which belongs to the DHH superfamily of phosphoesterases, has been proved as a key regulator in tumorigenesis. However, the role of h-prune in modulating HCC microenvironment is still poorly understood. We searched Pubmed and Google scholar by using the terms “h-prune”, “hepatocellular carcinoma”, and no relevant studies were found. (quality of evidence is not listed). During the process of our research, no studies reporting the association between h-prune and HCC.

Added value of our study

To our knowledge, our study is the first one to use clinical samples and genomic data from TCGA to evaluate the correlation of h-prune with HCC prognosis and its role in affecting HCC tumor microenvironment. We found that expression of h-prune is higher in HCC tumor cells than adjacent normal tissues, and higher expression of h-prune was correlated with poorer OS and DFS outcomes. By using RNAseq data, we also showed that the gene signatures of cell proliferation, DNA methylation and canonical Wnt signaling pathway were enriched in h-prune-high patients. We conducted somatic mutation analysis and the results demonstrated higher mutation burden of RB1 and RPS6KA3 in h-prune-high patients. Integrative analysis by using data from miRNAseq and methylation array revealed a strong correlation between h-prune expression and epigenetic changes.

Implications of all the available evidence

Our study has proved that the up-regulation of h-prune is associated with poorer survival outcomes in HCC patients. Moreover, our study also shows the correlation of h-prune expression with changes in HCC microenvironment. Our study provides encouraging support for h-prune as a potential prognostic biomarker and therapeutic target for HCC patients.

Atlas (TCGA). The clinical and histopathological features of h-prune in HCC tumor samples were assessed by immunohistochemistry (IHC). Moreover, we evaluated the correlation of h-prune expression with transcriptomic profiles, copy number variation (CNV), somatic mutations and epigenetic changes in HCC tissues. Compared to the previous studies focusing on the mechanism of h-prune in regulating tumor progression, our work is aimed at providing with evidences for using h-prune as a prognostic biomarker in risk stratification and a potential therapeutic target for HCC patients.

2. Methods and methods

2.1.1. Patients and samples

A total of 304 HCC patients (HUAXI dataset) undergoing hepatectomy between 2007 and 2012 in West China Hospital were included in this study. The diagnosis of HCC for each individual was confirmed by clinical features, laboratory parameters, macroscopic and histopathological alterations. Tissue microarrays were constructed as previously described [16]. Tumor staging classification was carried out according to the 7th AJCC TNM Staging for Liver and Intrahepatic Bile Duct Malignancies. The characteristics of tumor samples, including differentiation, size, number of nodules, vascular invasion and Ishak fibrosis score

of the adjacent liver tissue were evaluated by two pathologists specializing in hepatic diseases. The primary end point of this study was overall survival (OS), which was defined as the time from the date of surgery to the date of death without regard to the cause of death. The secondary end point was disease-free survival (DFS) defined as the time from the date of surgery to the time of the first event (recurrence, progression, death). Patients with no events were censored at the date of their last follow-up. Informed consent for the use of tissue for the purpose of biomedical research was provided by every individual patient, with the approval from the ethics committee of West China Hospital.

2.1.2. Evaluation of h-prune staining

Immunohistochemical (IHC) staining was performed as previously described [13] by using a specific anti-h-prune antibody (1/400, Abcam). Images of h-prune staining were viewed and captured using the NDP.view.2 software program. Slides were reviewed by two experienced pathologists who were blind to the clinical parameters. Expression of h-prune was recorded from 5 respective areas at 400× magnification from each immunostained HCC section by using a modified histological score (H-score) based both on the percentage of positively stained cells and on the intensity of staining, with a maximum score of 300. The mean value was used for further analyses.

2.1.3. Western blotting

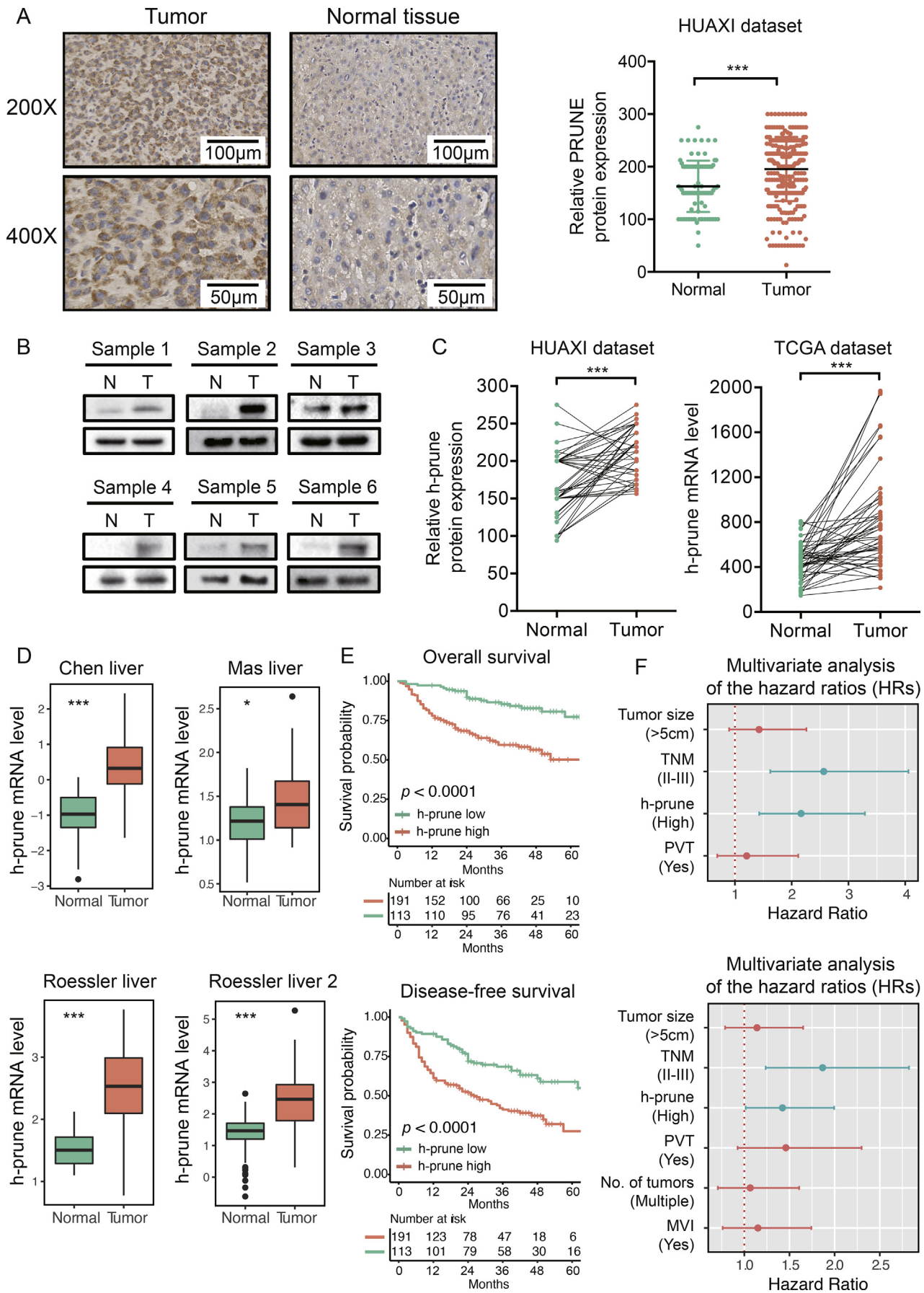
Western blot assays were conducted using standard techniques as previously described [17]. GAPDH antibody (Santa Cruz Biotechnology) was used as the control for whole-cell lysates. Antibody for h-prune was obtained from Abcam.

2.1.4. RNAseq gene expression analysis

Raw counts of gene expression from RNAseq were downloaded from the TCGA data portal (<https://portal.gdc.cancer.gov/>) for the differential gene expression analysis. Total raw read counts per gene were divided by the gene's maximum transcript length to represent a coverage depth estimate, which were then scaled to a total depth of 106 per sample and can be interpreted as transcripts per million (TPM) [18]. Statistical ranking for h-prune expression by the top and bottom quartiles were defined as h-prune-high and h-prune-low, respectively. Differential gene expression analysis between h-prune-high and h-prune-low patients across TCGA datasets was calculated using the R package edgeR, which determines the differential gene expression by accounting for variability through an over-dispersed Poisson model and moderating the degree of over-dispersion by Empirical Bayes methods [19]. Genes with counts per million (CPM) larger than 1 across at least 93 samples (half of all samples) were included for differential gene expression analysis. Genes with the adjusted *p* value < 0.05 and the absolute FC larger than 1.5 were considered to be statistically significant. Gene Ontology (GO) analysis on the aberrantly expressed genes between h-prune-high and h-prune-low patients was performed based on the Database for Annotation, Visualization and Integrated Discovery (DAVID, <https://david.ncicrf.gov/>) and gene set enrichment analysis (GSEA) as previously described [20]. GO terms with a false discovery rate (FDR) < 0.05 were considered statistically significant.

2.1.5. Mutation and copy number variation analysis

Significantly mutated genes (SMGs) were defined by running the Mutational Significance in Cancer (MuSiC Genome Suite) in different subtypes of HCC (h-prune-high vs. h-prune-low). MuSiC identifies genes with significantly higher mutation rates than the background mutation rate (BMR) to find SMGs across the entire sample population. The threshold for significance was a FDR of 0.1. Mutational spectra across the entire study population from the TCGA dataset were determined as previously described [3]. Copy number variation (CNV) data was downloaded from GDAC Firehose and separated into different datasets according to the expressions of h-prune. Investigation into significant amplification or deletion events in the regions of the genome was



conducted through the use of GISTIC 2.0, a revised computational program to identify somatic copy number alteration by investigating the frequency and amplitude of observed events [21]. Meanwhile, genes within the significant genomic regions were further analyzed to determine the overlay with those differentially expressed and identified from RNAseq.

2.1.6. Integration of gene expression and epigenetic change

To investigate the potential genes regulation by miRNA, we focused on aberrantly expressed miRNA (adjusted p value $< .05$, absolute FC > 1.5) and the significant differential gene selected from RNAseq between h-prune-high and h-prune-low patients. Since miRNAseq only provided the expression level of the stem loop, the stem loop's expression level was considered as the mature miRNA. The correlation between miRNA and the regulated genes was analyzed by TargetScan [22–26].

Preprocessed methylation data (mean beta values, level 3) were downloaded from Broad Firehose (<http://gdac.broadinstitute.org/>). Weighted Gene Co-Expression Network Analysis (WGCNA) [27] was conducted to identify groups of methylated genes (modules) involved in patients with different h-prune status (high vs. low) as previously described [28]. Genes in the modules showing statistically positive correlation with h-prune-high status were further analyzed to determine the overlay with those down-regulated in h-prune-high group and tumor-suppressor genes identified by Tumor Suppressor Gene database (TSGene) version 2.0 [29].

2.2. Statistical analysis

Statistical analyses and graphics were undertaken using R version 3.5.1. Student's t -test and Pearson χ^2 test were used for the univariate analyses where appropriate. Survival rates of expression level (high vs. low) were estimated by the Kaplan-Meier method with Rothman CIs. Survival curves were compared with the log-rank test. The hazard ratio (HR) and 95% CI associated with the expressions of h-prune were estimated through a multivariable Cox regression model adjusted for TNM stage (I vs. II–III), portal vein thrombus (no vs. yes), number of tumors (single vs. multiple), tumor size (≤ 5 cm vs. > 5 cm) and microvascular invasion (no vs. yes). A p value $< .05$ was considered statistically significant.

3. Results

3.1. h-prune is up-regulated in human HCC and associated with poorer survival outcomes

To investigate the clinical relevance of h-prune in HCC, the expression of h-prune was evaluated in TMA containing 304 HCC samples and matched adjacent normal tissues ($n = 50$). IHC results demonstrated increased expression of h-prune in HCC samples compared with adjacent normal tissues (Fig. 1A). In addition, h-prune expression in 6 human HCC tissues and paired normal tissues was detected by Western blot analysis. In spite of inter-individual variations, h-prune was found to be significantly up-regulated in HCC tissues (Fig. 1B). Meanwhile, paired t -test showed h-prune expression was up-regulated in HCC tissues compared with matched adjacent normal tissues, which was further validated by using TCGA datasets (Fig. 1C). Moreover, the up-regulated expression of h-prune in HCC was verified

by gene expression analysis based on 4 Oncomine datasets (Fig. 1D). By using X-tile software [30] to find the best cut-off point to parse patients into subsets with distinguishing survival outcomes based on h-prune expression, we were able to stratified 304 HCC patients into h-prune-high ($n = 191$) and h-prune-low ($n = 113$) subgroups. It was found that higher expression of h-prune was correlated with poorer OS and DFS outcomes (Fig. 1E). Consistent with the results in HUAXI dataset, patients with higher h-prune expression in TCGA dataset also have poorer survival outcomes (Supplementary Fig. S1). On the other hand, multivariate analysis showed that h-prune expression was an independent risk factor for both OS and DFS (Fig. 1F). Taken together, these results show that h-prune is frequently up-regulated in HCC tissue, suggesting that h-prune may play a role in HCC progression, thus leading to poorer survival outcomes.

3.2. Potential mechanism of h-prune in regulating the progression of HCC

To elucidate whether h-prune could play a role in promoting HCC occurrence, a RNAseq gene expression analysis was performed to compare the gene expression profiles of h-prune-high and -low groups. A total of 2006 up-regulated genes (≥ 1.5 -fold) and 1972 down-regulated genes (≥ 1.5 -fold) were detected in h-prune-high group (h-prune-low group as reference, Fig. 2A). GO analysis revealed changes in gene sets related to cell proliferation, DNA methylation and canonical Wnt signaling pathway in patients with higher expression of h-prune (Fig. 2B). In order to gain further insight into the biologic pathways involved in HCC pathogenesis stratified by h-prune expression level, GSEA analysis was then performed. Enrichment plots of GSEA also showed that the gene signatures of cell proliferation, DNA methylation and canonical Wnt signaling pathway were enriched in h-prune-high patients. It can be concluded that there is a strong correlation between the expression of these genes and h-prune up-regulation. Considering that h-prune has been proved to act as an activator of the Wnt signaling [11,31], these facts highly indicate the potential function of h-prune as a tumor promoter in HCC by activating tumor cell proliferation through Wnt signaling pathway and inducing the methylation of tumor suppressor genes.

3.3. Mutational event and CNV analysis in patients with high vs. low expression of h-prune

Previous genetic profiling studies have provided an accurate landscape of the driver gene mutations in HCC [3]. Based on these facts, we evaluated the correlation of h-prune expression with distinct mutational profiles characterized for HCC. It was found that h-prune-high tumors had statistically higher mutations burdens in RPS6KA3 (Fig. 3A), which has been proved to participate in the process of cell proliferation [32]. Meanwhile, higher mutation burdens in RB1 (Fig. 3A), which is a well-known tumor suppressor gene [33], could also be detected in tumors with higher h-prune expression. This finding indicates a potential gain of function associated with RPS6KA3 and RB1 mutations, which contributes to h-prune overexpression.

To explore the association between CNV and h-prune expression, we used GISTIC 2.0 to analyze the alteration of chromosome regions. We found that a large number of cytobands were either significantly amplified or deleted regardless of the influence by h-prune expression (Fig. 3B). Compared with h-prune-low subgroup, a total of 402 genes were within the chromosome regions with copy number significantly

Fig. 1. h-prune is upregulated in HCC tissues and predicts poorer survival outcomes. (A) representative IHC staining of h-prune in HCC and adjacent normal tissues (left panel); scale bar, 50 μ m. The relative protein level of h-prune is significantly higher in HCC tissues than in adjacent normal tissue (right panel). Data represent the mean \pm SD. ***, $p < .001$. (B) Western blot analysis of h-prune expression in HCC tissues and patient-matched adjacent normal tissues. (C) the relative level of h-prune expression is higher in HCC than patient-matched adjacent normal tissues (left), which is further validated by TCGA dataset (right). ***, $p < .001$. (D) the relative mRNA expression of h-prune in four Oncomine datasets. Data represent the mean \pm SD. *, $p < .05$; ***, $p < .001$. (E) Higher expression of h-prune predicts poorer survival outcomes in patients with HCC. (F) Multivariable Cox regression analysis shows that h-prune is an independent risk factor for both OS (upper panel) and DFS (lower panel). Independent prognostic factors, including h-prune expression and other clinical parameters, were assessed using the multivariate Cox proportional hazards model among the variables found to be significant using univariate analysis. The HRs are presented as the means with 95% confidence interval. Differences with $p < .05$ (Tiffany) were considered significant.

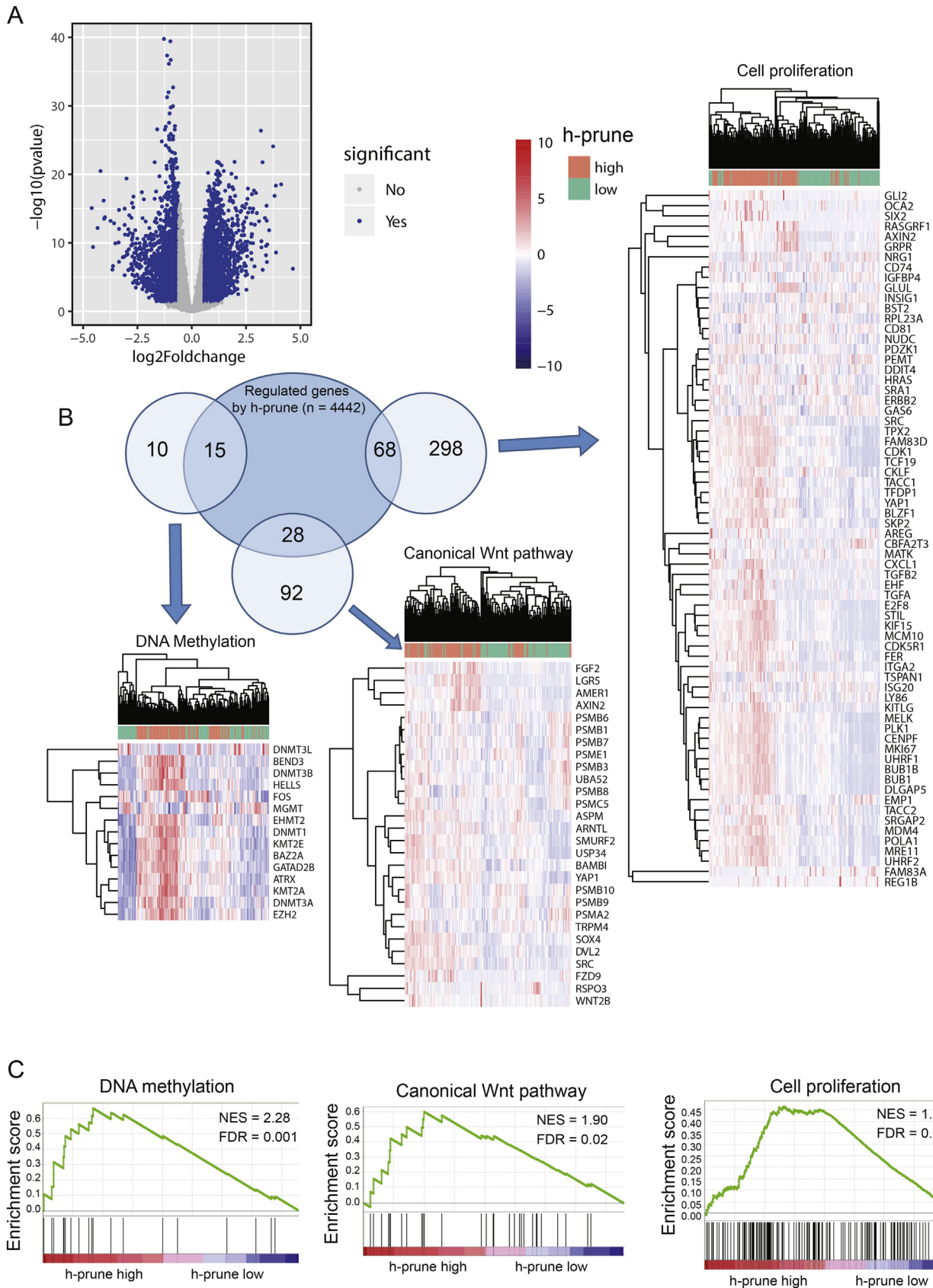


Fig. 2. Identifying differentially expressed genes between h-prune-high and -low patients. (A) Volcano plot of differential gene profiles between h-prune-high and -low groups. (B) GO analysis by DAVID shows that genes involved in cell proliferation, canonical Wnt pathway and DNA methylation are enriched in h-prune-high patients. Venn plot demonstrates the overlapping between differentially expressed genes and genes participating in different biological processes. Each circle in the Venn plot represents one set and the number in the overlaid area represents the common genes between the sets. (C) GSEA analysis as a validation for the gene enrichment results from Fig. 2B.

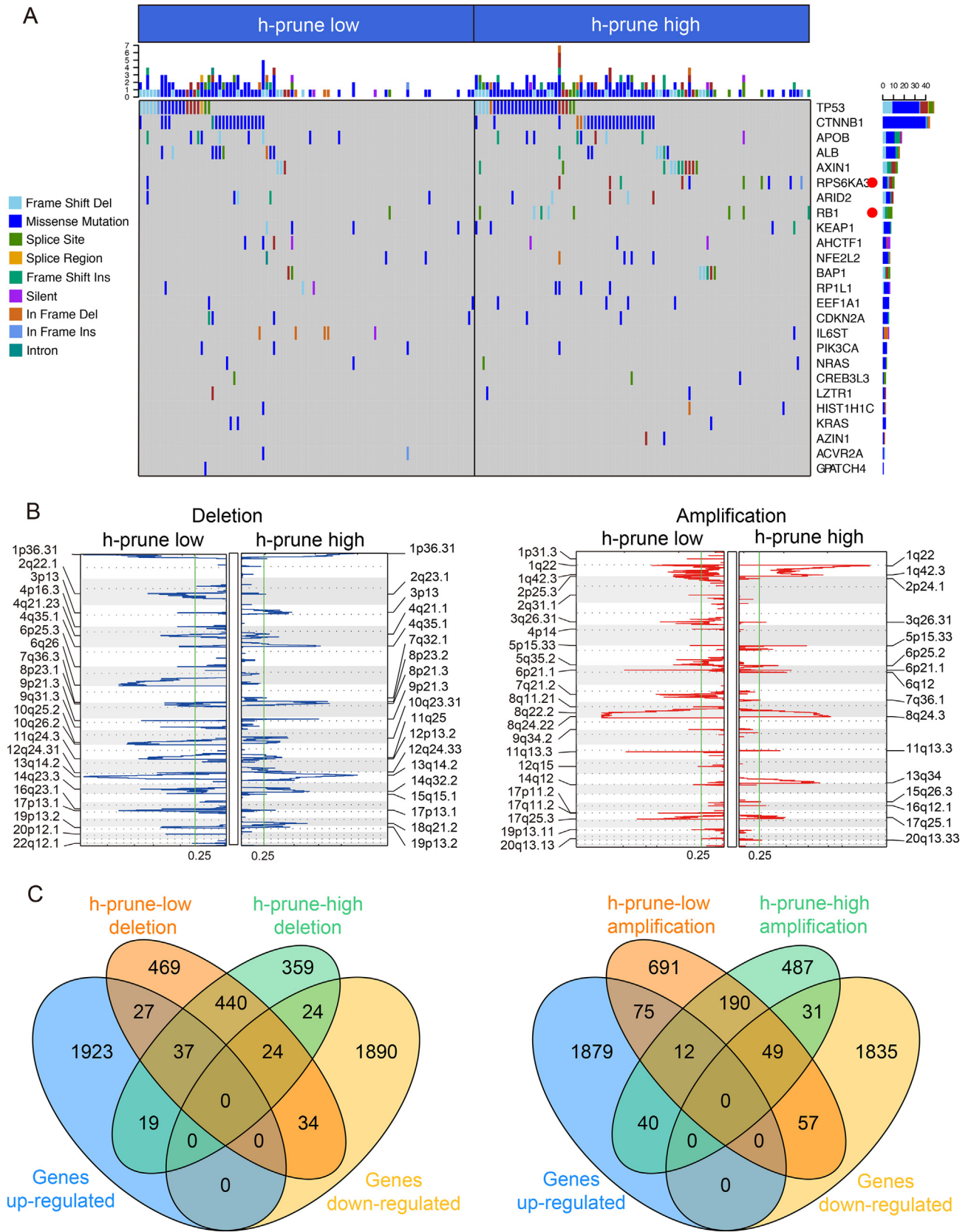
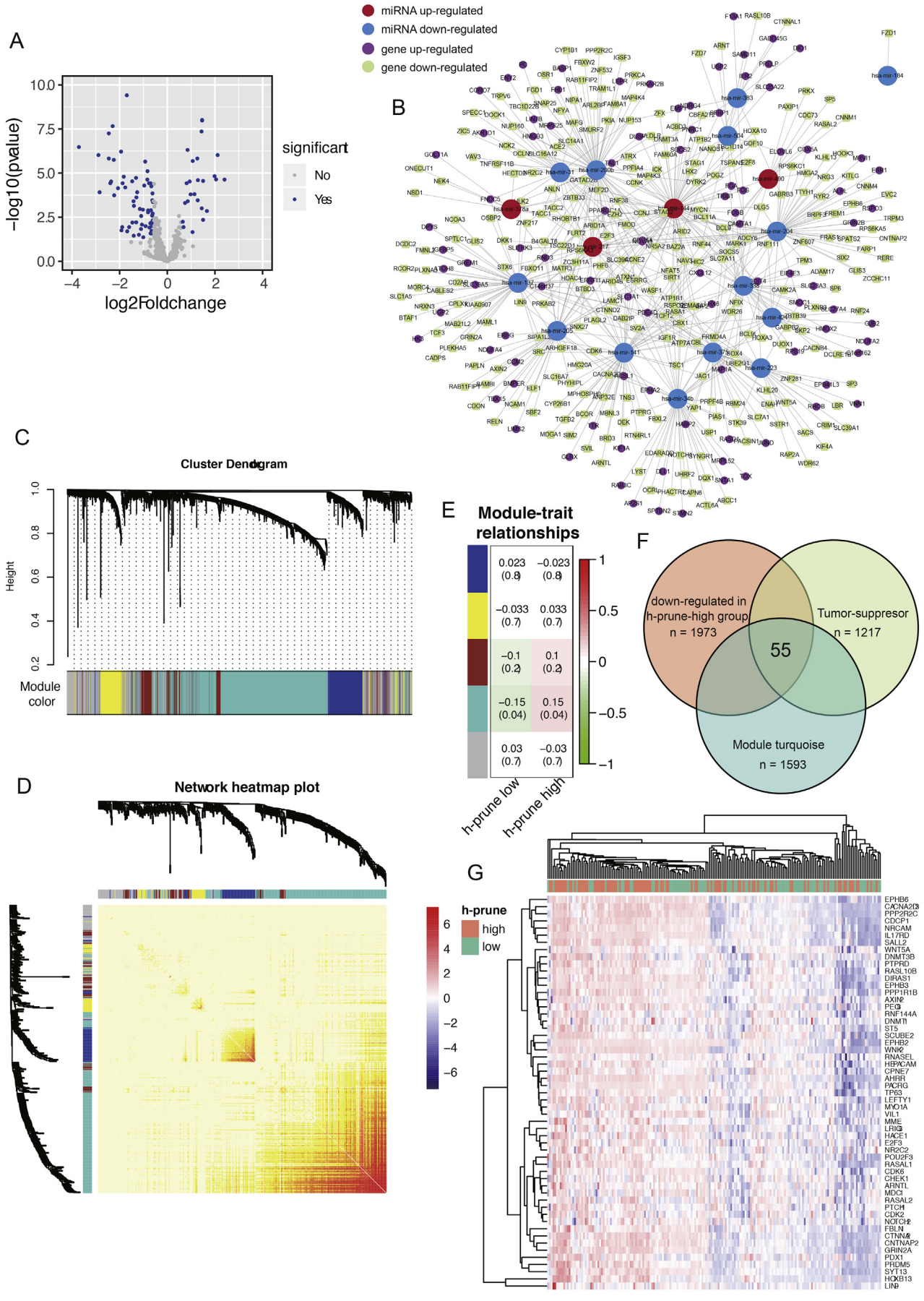


Fig. 3. Association between h-prune and mutational signatures, CNV in HCC. (A) Significantly mutated genes in HCC subsets stratified by h-prune expression. Red dot, $p < .05$. (B) GISTIC2.0 analysis identified recurrent somatic copy number alterations in different HCC subsets stratified by h-prune expression. Venn diagrams demonstrating the number of genes within genomic regions showing significant amplification or deletion, as well as the overlay with significant genes identified from RNAseq. Each circle in the Venn diagram represents one set and the number in the overlaid area represents the common genes between the sets.



deleted in h-prune-high patients (Fig. 3C, left panel). After overlaid with the significantly differentially expressed genes identified by RNAseq, 43 genes within the deletion regions in h-prune-high group showed the concordant expression pattern in RNAseq, which implied that the differential expression of these genes may be partially owing to copy number deletions. On the other hand, the number of genes within the aberrantly amplified regions in h-prune-high subgroup was 558 (Fig. 3C, right panel), among which 71 genes were also identified as statistically dys-regulated according to RNAseq, suggesting that differential expression of these genes may be partially due to the copy number amplifications. Despite a small number of genes exhibiting concordance between RNAseq and CNV results regardless of amplification and deletion, the majority of the aberrantly expressed genes identified from RNAseq in h-prune-high patients were not affected by CNV, indicating the independence of aberrant gene expression from CNV in patients with higher h-prune expression.

3.4. Correlation of miRNAs with h-prune expression

microRNAs (abbreviated miRNAs) are small non-coding RNAs (about 22 nt) that function in targeting mRNAs for cleavage and post-transcriptional regulation [34]. It has been proved that dys-regulation of miRNA expression is a key step in HCC carcinogenesis [35]. In our work, we sought to evaluate the genes potentially regulated by miRNA after the up-regulation of h-prune. Therefore, TargetScan was used to predict the relationship between miRNAs and their target genes. A total of 25 up-regulated miRNAs (≥ 1.5 -fold) and 73 down-regulated miRNAs (≥ 1.5 -fold) were detected in h-prune-high group (h-prune-low group as reference, Fig. 4A). By using TargetScan, we found that a total of 568 pairs of miRNA-mRNA interaction were identified, among which 440 pairs owned genes highly down-regulated in HCC with higher h-prune expression (Fig. 4B). Surprisingly, hsa-mir-200b negatively regulated the expression of over 50 genes. Meanwhile, 97 genes were negatively regulated by more than one miRNA. The interaction network showed oncogenes potentially regulated by miRNA, including BCL9, CDK6, SOX4 and NOTCH1 [36–39]. However, this network also demonstrated that the expression of tumor suppressor genes, including ARID1A and CAMTA1 [40,41], were also potentially modulated by miRNAs. These results suggest the feed-back loop existing in HCC carcinogenesis regulated by miRNA in h-prune-high patients.

3.5. Analysis on the potential epigenetic changes correlated with h-prune expression

DNA methylation is thought to be another epigenetic factor regulating gene expression. The occurrence of DNA methylation in CpG island of gene promoters will lead to gene expression suppression [42]. The dysregulation of DNA methylation has been proved to be significantly correlated with HCC progression [43–45]. Moreover, genes involved in DNA methylation were enriched in h-prune-high patients according to the GSEA analysis in present study. These facts highly suggested that up-regulation of h-prune might contribute to the epigenetic modification of cancer-related genes. In order to evaluate DNA methylation patterns in h-prune-low and -high patients, we used WGCNA to cluster methylated genes into different co-methylation modules. The network and the identified modules were depicted in Fig. 4C and D. Each module was assigned with a unique color identifier, with the remaining poorly connected genes colored gray. Notably, only the turquoise module showed a statistically positive correlation with h-prune-high status

(Bonferroni threshold of $p < .05$, Fig. 4E). In order to find significant target genes methylated after the up-regulation of h-prune, we overlaid tumor suppressor genes with turquoise module and down-regulated genes identified in h-prune-high patients. The results demonstrated that methylation status of 55 tumor suppressor genes were potentially affected by h-prune up-regulation (Fig. 4F). A distinct beta value distribution of these 55 genes was found between two HCC subtypes, in which h-prune-high tumors were enriched with higher beta values (Fig. 4G).

4. Discussion

Functioning as a phosphoesterases, h-prune exerts ability in promoting carcinogenesis by its phosphodiesterase (PDE) activity. At this moment, studies focusing on h-prune as a prognosis biomarker in cancers are still limited. To our knowledge, this study is the first one to evaluate the prognostic value of h-prune in HCC patients. Consistent with previous studies on breast cancer and colorectal liver metastasis [12,15], the expression of h-prune was predominantly located in the cytoplasm of tumor cells in HCC tissues. Moreover, higher h-prune expression in HCC tumor cells was also correlated with poorer survival outcomes. By analyzing the differentially expressed genes between h-prune-low and -high HCC tumors in TCGA dataset, we found that h-prune-high tumors were enriched with genes involved in cell proliferation and Wnt signaling pathway. Since aberrant activation of Wnt pathway has been proved to be involved in HCC progression [46], these findings have provided with evidence of h-prune as an oncogene in hepatocarcinogenesis.

The retinoblastoma gene RB1, which is the first identified tumor suppressor gene, has been proved to be involved in the regulation of cell cycle progression, DNA replication, and terminal differentiation [47]. The mutation of RB1 can be found in almost all familial and sporadic forms of retinoblastoma and a variety of other human cancers at variable frequencies, which contributes to the inactivation of its gene product pRB in compromising the ability of cells to exit the cell cycle and places normal cells in a state of high susceptibility to oncogenic proliferation [33]. In this study, we observed that the proportion of HCC patients with RB1 mutations in h-prune-high group was statistically significant higher than that in h-prune-low group, indicating a potential mechanism of the suppression of pRB by h-prune in regulating HCC cell proliferation, which leads to oncogenic proliferation of HCC tumor cells.

Numerous studies have shown that miRNAs can manipulate tumorigenesis. During the process of tumorigenesis, mature miRNA is incorporated into a large protein complex called RNA-induced silencing complex (RISC), which cleaves the target mRNA or induces translational repression [48–50]. After identifying significant miRNAs potentially regulated by h-prune expression, we found that the expression of hsa-mir-34b, which has been proved to be a tumor suppressor in Burkitt lymphoma [51], was also down-regulated in h-prune-high HCC patients. In addition, the expression of hsa-mir-223, which shows negative correlation with the tumor suppressor gene SEL1L in human pancreatic ductal adenocarcinoma [52], was up-regulated in h-prune-high group. Moreover, there were multiple synchronizations between the expressions of miRNAs and their target genes. These results highly suggest the complicated regulatory network by miRNA expression along with the up-regulation of h-prune.

Besides the regulation of miRNA, DNA methylation resulting in transcriptional silencing of tumor suppressor genes also has been well established as a significant epigenetic aberration in cancers [53]. Thus,

Fig. 4. Integration of epigenetic change and gene expression between h-prune-high and -low patients. (A) Volcano plot of differentially expressed miRNAs between h-prune-high and -low groups. (B) Regulation of gene expression by miRNA plot as network in cytoscape. (C) Dendrogram indicating expression of different gene modules in patients involved in WGCNA analysis. (D) Pearson correlations between expression profiles of all pairs of genes were transformed into network connection strengths (denoted by intensity of red color). (E) Correlation between module eigengenes and the expression level of the h-prune (low vs. high). (F) Venn diagrams demonstrating the number of genes within module turquoise, as well as the overlay with down-regulated genes identified from RNAseq and tumor suppressor genes. (G) Hierarchical clustering showing beta values of the 55 genes identified from Fig. 4F.

tumor suppressor gene reactivation by reversing the hypermethylation status has become a hot spot in targeted cancer therapy. Recently, clinical development of hypomethylating agents, including azacitidine and decitabine, has been achieved in hematology, suggesting the further application of hypomethylating agents in other cancer types [54]. Considering that genes participating in DNA methylation process were enriched in HCC patients with higher h-prune expression, analyzing the DNA methylation status is of great clinical value in identifying the potential treatment target in patients with positive h-prune expression. This study shows that a large number of tumor suppressor genes exhibit higher methylation status in h-prune-high patients compared with those in h-prune-low patients, indicating the existence of multiple hypomethylating agent targets. Further research will be inspired to promote the application of demethylation agents on h-prune-positive HCC patients.

In summary, this study has highlighted the clinical value of h-prune in predicting the prognosis of HCC patients and its potential role in affecting gene expression, somatic mutation and epigenetic modifications. These results suggest the underlying mechanism contributing to the poorer survival outcomes of HCC patients with higher h-prune expression. Moreover, this study has provided potentially practical management options for future clinical trials on h-prune targeted therapy for HCC patients.

Supplementary data to this article can be found online at <https://doi.org/10.1016/j.ebiom.2019.01.001>.

Funding sources

This work was supported by grants from the Natural Science Foundation of China (81872004, 81800564, 81770615, 81700555, 81672882 and 81502441), the Science and Technology Support Program of Sichuan Province (2017SZ0003, 2018SZ0115) and the Science and Technology Program of Tibet Autonomous Region (XZ201801-GB-02).

Declarations of interests

The authors have declared that no competing interest exists.

Authors contribution

Kefei Yuan and Yong Zeng designed this research; Haotian Liao and Lin Xu performed the IHC experiment and western blotting; Mingheng Liao, Xiaokai Yan, Bo Ren and Zexin Zhu performed data collection and pre-processing of data; Haotian Liao and Mingheng Liao analyzed both experimental and genomics data and wrote the manuscript.

Acknowledgements

We thank the TCGA working group for generating publicly available data. We are most grateful for Core Facility of West China Hospital for their technique support.

References

- Chen W, Zheng R, Baade PD, Zhang S, Zeng H, Bray F, et al. Cancer statistics in China, 2015. *CA Cancer J Clin* 2016;66(2):115–32.
- EASL Clinical Practice Guidelines: management of hepatocellular carcinoma. *J Hepatol* 2018;69(1):182–236.
- Comprehensive and integrative genomic characterization of hepatocellular carcinoma. *Cell* 2017;169(7):1327–41.e23.
- Sung WK, Zheng H, Li S, Chen R, Liu X, Li Y, et al. Genome-wide survey of recurrent HBV integration in hepatocellular carcinoma. *Nat Genet* 2012;44(7):765–9.
- Woo HG, Wang XW, Budhu A, Kim YH, Kwon SM, Tang ZY, et al. Association of TP53 mutations with stem cell-like gene expression and survival of patients with hepatocellular carcinoma. *Gastroenterology* 2011;140(3):1063–70.
- Cooney JD, Aguiar RC. Phosphodiesterase 4 inhibitors have wide-ranging activity in B-cell malignancies. *Blood* 2016;128(25):2886–90.
- Loeb S, Folkvaljon Y, Lambe M, Robinson D, Garmo H, Ingvar C, et al. Use of phosphodiesterase type 5 inhibitors for erectile dysfunction and risk of malignant melanoma. *JAMA* 2015;313(24):2449–55.
- Loeb S, Folkvaljon Y, Robinson D, Schlomm T, Garmo H, Stattin P. Phosphodiesterase type 5 inhibitor use and disease recurrence after prostate cancer treatment. *Eur Urol* 2016;70(5):824–8.
- D'Angelo A, Garzia L, Andre A, Carotenuto P, Aglio V, Guardiola O, et al. Prune cAMP phosphodiesterase binds nm23-H1 and promotes cancer metastasis. *Cancer Cell* 2004;5(2):137–49.
- Kobayashi T, Hino S, Oue N, Asahara T, Zollo M, Yasui W, et al. Glycogen synthase kinase 3 and h-prune regulate cell migration by modulating focal adhesions. *Mol Cell Biol* 2006;26(3):898–911.
- Carotenuto M, De Antonellis P, Liguori L, Benvenuto G, Magliulo D, Alonzi A, et al. H-Prune through GSK-3beta interaction sustains canonical WNT/beta-catenin signaling enhancing cancer progression in NSCLC. *Oncotarget* 2014;5(14):5736–49.
- Hashimoto M, Kobayashi T, Tashiro H, Arihiro K, Kikuchi A, Ohdan H. H-Prune is associated with poor prognosis and epithelial-mesenchymal transition in patients with colorectal liver metastases. *Int J Cancer* 2016;139(4):812–23.
- Hwang D, Zhao Y, Liu H, Kabanov A, Gershon T, Sokolsky M. MBRS-53. enhanced efficacy of Nano-formulated Vismodegib shows the potential for polyoxazoline micelles to improve drug delivery to brain tumors. *Neuro Oncol* 2018;20(suppl_2)(i139-i40).
- Nambu J, Kobayashi T, Hashimoto M, Tashiro H, Sugino K, Shimamoto F, et al. H-prune affects anaplastic thyroid cancer invasion and metastasis. *Oncol Rep* 2016;35(6):3445–52.
- Zollo M, Andre A, Cossu A, Sini MC, D'Angelo A, Marino N, et al. Overexpression of h-prune in breast cancer is correlated with advanced disease status. *Clin Cancer Res* 2005;11(1):199–205.
- Xie K, Xu L, Wu H, Liao H, Luo L, Liao M, et al. OX40 expression in hepatocellular carcinoma is associated with a distinct immune microenvironment, specific mutation signature, and poor prognosis. *Oncotarget* 2018;7(4):e1404214.
- Xiong H, Hong J, Du W, Lin YW, Ren LL, Wang YC, et al. Roles of STAT3 and ZEB1 proteins in E-cadherin down-regulation and human colorectal cancer epithelial-mesenchymal transition. *J Biol Chem* 2012;287(8):5819–32.
- Rooney MS, Shukla SA, Wu CJ, Getz G, Hacohen N. Molecular and genetic properties of tumors associated with local immune cytolytic activity. *Cell* 2015;160(1–2):48–61.
- Robinson MD, McCarthy DJ, Smyth GK. edgeR: a Bioconductor package for differential expression analysis of digital gene expression data. *Bioinformatics* 2010;26(1):139–40.
- Liao HT, Huang JW, Lan T, Wang JJ, Zhu B, Yuan KF, et al. Identification of the aberrantly expressed lncRNAs in hepatocellular carcinoma: a bioinformatics analysis based on RNA-sequencing. *Sci Rep* 2018;8(1):5395.
- Mermel CH, Schumacher SE, Hill B, Meyerson ML, Beroukhim R, Getz G. GISTIC2.0 facilitates sensitive and confident localization of the targets of focal somatic copy-number alteration in human cancers. *Genome Biol* 2011;12(4):R41.
- Agarwal V, Bell GW, Nam JW, Bartel DP. Predicting effective microRNA target sites in mammalian mRNAs. *Elife* 2015;4.
- Friedman RC, Farh KK, Burge CB, Bartel DP. Most mammalian mRNAs are conserved targets of microRNAs. *Genome Res* 2009;19(1):92–105.
- Garcia DM, Baek D, Shin C, Bell GW, Grimson A, Bartel DP. Weak seed-pairing stability and high target-site abundance decrease the proficiency of Isy-6 and other microRNAs. *Nat Struct Mol Biol* 2011;18(10):1139–46.
- Grimson A, Farh KK, Johnston WK, Garrett-Engle P, Lim LP, Bartel DP. MicroRNA targeting specificity in mammals: determinants beyond seed pairing. *Mol Cell* 2007;27(1):91–105.
- Lewis BP, Burge CB, Bartel DP. Conserved seed pairing, often flanked by adenosines, indicates that thousands of human genes are microRNA targets. *Cell* 2005;120(1):15–20.
- Langfelder P, Horvath S. WGCNA: an R package for weighted correlation network analysis. *BMC Bioinform* 2008;9:559.
- Gargalovic PS, Imura M, Zhang B, Gharavi NM, Clark MJ, Pagnon J, et al. Identification of inflammatory gene modules based on variations of human endothelial cell responses to oxidized lipids. *Proc Natl Acad Sci U S A* 2006;103(34):12741–6.
- Zhao M, Kim P, Mitra R, Zhao J, Zhao Z. TSGene 2.0: an updated literature-based knowledgebase for tumor suppressor genes. *Nucleic Acids Res* 2016;44(D1):D1023–31.
- Camp RL, Dolled-Filhart M, Rimm DL. X-tile: a new bio-informatics tool for biomarker assessment and outcome-based cut-point optimization. *Clin Cancer Res* 2004;10(21):7252–9.
- Freeman J, Smith D, Latinkic B, Ewan K, Samuel L, Zollo M, et al. A functional connectome: regulation of Wnt/TCF-dependent transcription by pairs of pathway activators. *Mol Cancer* 2015;14:206.
- Anjum R, Blenis J. The RSK family of kinases: emerging roles in cellular signalling. *Nat Rev Mol Cell Biol* 2008;9(10):747–58.
- Dyson NJ. RB1: a prototype tumor suppressor and an enigma. *Genes Dev* 2016;30(13):1492–502.
- Bartel DP. MicroRNAs: genomics, biogenesis, mechanism, and function. *Cell* 2004;116(2):281–97.
- Yang N, Ekanem NR, Sakyi CA, Ray SD. Hepatocellular carcinoma and microRNA: new perspectives on therapeutics and diagnostics. *Adv Drug Deliv Rev* 2015;81:62–74.
- Tiwari N, Tiwari VK, Waldmeier L, Balwiercz PJ, Arnold P, Pachkov M, et al. Sox4 is a master regulator of epithelial-mesenchymal transition by controlling Ezh2 expression and epigenetic reprogramming. *Cancer Cell* 2013;23(6):768–83.

- [37] Takada K, Zhu D, Bird GH, Sukhdeo K, Zhao JJ, Mani M, et al. Targeted disruption of the BCL9/beta-catenin complex inhibits oncogenic Wnt signaling. *Sci Transl Med* 2012;4(148):148ra17.
- [38] Dail M, Wong J, Lawrence J, O'Connor D, Nakitandwe J, Chen SC, et al. Loss of oncogenic Notch1 with resistance to a PI3K inhibitor in T-cell leukaemia. *Nature* 2014;513(7519):512–6.
- [39] Asghar U, Witkiewicz AK, Turner NC, Knudsen ES. The history and future of targeting cyclin-dependent kinases in cancer therapy. *Nat Rev Drug Discov* 2015;14(2):130–46.
- [40] Wiegand KC, Shah SP, Al-Agha OM, Zhao Y, Tse K, Zeng T, et al. ARID1A mutations in endometriosis-associated ovarian carcinomas. *N Engl J Med* 2010;363(16):1532–43.
- [41] Schraivogel D, Weinmann L, Beier D, Tabatabai G, Eichner A, Zhu JY, et al. CAMTA1 is a novel tumour suppressor regulated by miR-9/9* in glioblastoma stem cells. *EMBO J* 2011;30(20):4309–22.
- [42] Dor Y, Cedar H. Principles of DNA methylation and their implications for biology and medicine. *Lancet* 2018;392(10149):777–86.
- [43] Yoshikawa H, Matsubara K, Qian GS, Jackson P, Groopman JD, Manning JE, et al. SOCS-1, a negative regulator of the JAK/STAT pathway, is silenced by methylation in human hepatocellular carcinoma and shows growth-suppression activity. *Nat Genet* 2001;28(1):29–35.
- [44] Park IY, Sohn BH, Yu E, Suh DJ, Chung YH, Lee JH, et al. Aberrant epigenetic modifications in hepatocarcinogenesis induced by hepatitis B virus X protein. *Gastroenterology* 2007;132(4):1476–94.
- [45] Mudbhary R, Hoshida Y, Chernyavskaya Y, Jacob V, Villanueva A, Fiel MI, et al. UHRF1 overexpression drives DNA hypomethylation and hepatocellular carcinoma. *Cancer Cell* 2014;25(2):196–209.
- [46] Hoshida Y, Toffanin S, Lachenmayer A, Villanueva A, Minguez B, Llovet JM. Molecular classification and novel targets in hepatocellular carcinoma: recent advancements. *Semin Liver Dis* 2010;30(1):35–51.
- [47] Du W, Pogoriler J. Retinoblastoma family genes. *Oncogene* 2006;25(38):5190–200.
- [48] Bartel DP. MicroRNAs: target recognition and regulatory functions. *Cell* 2009;136(2):215–33.
- [49] Chendrimada TP, Gregory RI, Kumaraswamy E, Norman J, Cooch N, Nishikura K, et al. TRBP recruits the Dicer complex to Ago2 for microRNA processing and gene silencing. *Nature* 2005;436(7051):740–4.
- [50] Hutvagner G, Zamore PD. A microRNA in a multiple-turnover RNAi enzyme complex. *Science* 2002;297(5589):2056–60.
- [51] Leucci E, Cocco M, Onnis A, De Falco G, van Cleef P, Bellan C, et al. MYC translocation-negative classical Burkitt lymphoma cases: an alternative pathogenetic mechanism involving miRNA deregulation. *J Pathol* 2008;216(4):440–50.
- [52] Liu Q, Chen J, Wang J, Amos C, Killary AM, Sen S, et al. Putative tumor suppressor gene SEL1L was downregulated by aberrantly upregulated hsa-mir-155 in human pancreatic ductal adenocarcinoma. *Mol Carcinog* 2014;53(9):711–21.
- [53] Jones PA, Baylin SB. The epigenomics of cancer. *Cell* 2007;128(4):683–92.
- [54] Navada SC, Steinmann J, Lubbert M, Silverman LR. Clinical development of demethylating agents in hematology. *J Clin Invest* 2014;124(1):40–6.